Latitudinal structure of outer Io plasma torus

Michel Moncuquet, Fran Bagenal, Nicole Meyer

Latitudinal structure of outer Io plasma torus

Michel Moncuquet
Département de Recherche Spatiale, Observatoire de Paris, Meudon, France

Fran Bagenal
Department of Astrophysical, Planetary and Atmospheric Sciences, University of Colorado, Boulder, Colorado, USA

Nicole Meyer-Vernet
Département de Recherche Spatiale, Observatoire de Paris, Meudon, France

Received 8 April 2001; revised 19 July 2001; accepted 2 August 2001; published 28 September 2002.

[1] We present a model of the latitudinal structure of the Io plasma torus (IPT), which is able to explain Ulysses results and to reconcile several in situ data sets. Basically, the observed temperature inversion and the polytropic law are due to "velocity filtration" of particles having non-Maxwellian velocity distributions. This mechanism acts as a high-pass filter for particle energies if the particles are confined in an attractive monotonic potential well. These conditions are met in the IPT, where the attractive potential is due to the centrifugal force that confines plasma ions since the plasma is corotating with Jupiter, whereas electrons are confined by an ambipolar electric field preserving electric neutrality, and the electron velocity distribution is known to have a suprathermal tail. The suprathermal electron population has a velocity distribution that decreases with increasing energy as a power law, as is frequently observed in space plasmas, and the velocity distribution can be conveniently modeled with a "kappa" function [*Meyer-Vernet et al.*, 1995]. Adopting such a kappa distribution for the electrons and for all ion species detected in the torus and including temperature anisotropy, we construct a collisionless kinetic model based on the so-called "bi-kappa distributions" to calculate the latitudinal structure. Following *Bagenal* [1994], we adopt the nearly equatorial data set from Voyager 1 to represent empirically the radial structure. The model reconciles the Voyager 1 and 2 and Ulysses observations and demonstrates that these data sets possess similar latitudinal and radial variations of the IPT densities and temperatures. This model also generates a radial ion temperature profile past ~7.5 Jovian radii, which is compatible with a quasiadiabatic radial temperature decrease at the torus equator. *INDEX TERMS:* 5780 Planetology: Fluid Planets: Tori and exospheres; 6218 Planetology: Solar System Objects: Jovian satellites; 2756 Magnetospheric Physics: Planetary magnetospheres (5443, 5737, 6030); *KEYWORDS:* Io, plasma, torus, kinetic, model, confinement

Citation: Moncuquet, M., F. Bagenal, and N. Meyer-Vernet, Latitudinal structure of outer Io plasma torus, *J. Geophys. Res.*, *107*(A9), 1260, doi:10.1029/2001JA900124, 2002.

1. Introduction

[2] The Io plasma torus (IPT) in the inner Jovian magnetosphere contains charged particles confined by the action of the strong magnetic field and of the fast rotation of Jupiter and ultimately supplied by the innermost Galilean satellite Io. The spatial distribution has a toroidal shape with inner and outer radii of ~5 and 12 R_J (Jovian radii), respectively, and vertical thickness of 3 R_J. Since different spacecraft have taken in situ measurements on at least five traversals of the torus, the IPT constitutes a valuable natural laboratory for comparing in situ measurements with remote plasma sensing techniques, for testing our understanding of the basic physics at work in the IPT, and for providing a reliable model of its large-scale structure. Such a model is also a key requirement for understanding Jupiter as one of brightest radio sources in the sky.

[3] The need for a new plasma torus model, especially its latitudinal structure, was driven by the Ulysses radio spectra acquired in 1992. In contrast to the Voyager 1 or Galileo spacecraft, Ulysses passed through the IPT on a north-to-south trajectory (see Figure 1) and nearly tangentially to a magnetic shell ($L \approx 8\ R_J$), which allowed, for the first time, the determination of the electron density and temperature along the magnetic field. The principal and most unexpected result was that the electron temperature increased substantially with magnetic latitude (doubling over 7° of latitude) and was anticorrelated with the

0148-0227/02/2001JA900124

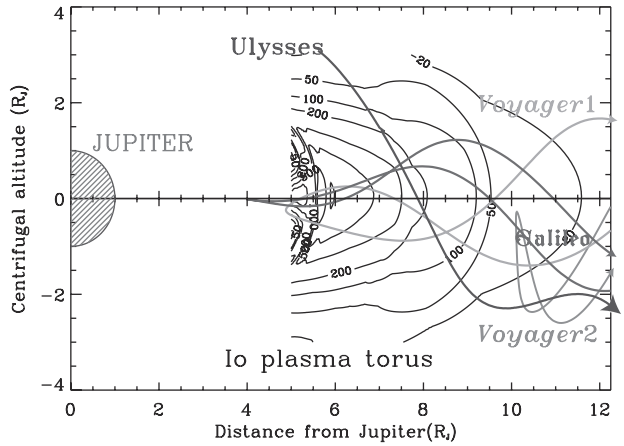

Figure 1. The trajectories of four spacecraft that have flown through the Io torus: Voyager 1 (green), Voyager 2 (pink), Ulysses (red), and Galileo's initial orbit (blue). The contours show electron density from the model of *Bagenal* [1994] (isotropic case with O_6 magnetic field model and no current sheet). See color version of this figure at back of this issue.

electron density, obeying a polytropic law with an index of ~0.48 [*Moncuquet et al.*, 1995; *Meyer-Vernet et al.*, 1995]. This substantial variation of electron temperature was incompatible with previous IPT models [*Divine and Garrett*, 1983; *Bagenal*, 1994]. In addition, the observed latitudinal variation in electron temperature raises the question of whether the temperature of the ions varies similarly.

[4] In this paper we find that even if we adopt multiple (Maxwellian) velocity distributions (core plus halo), the latitudinal variation in temperature and the equatorial confinement of the electrons is underestimated by the model when compared with the Ulysses observations. Introducing a temperature anisotropy at the equator helped confine the plasma to the equator but yielded a temperature which decreases with latitude, contrary to Ulysses' observations. For these reasons we developed a new model.

2. Latitudinal Distribution of Electrons

2.1. Velocity Filtration

[5] In order to explain the increase in electron temperature with latitude and anticorrelation with density observed by Ulysses along its north-south traversal of the torus, *Meyer-Vernet et al.* [1995] invoked non-Maxwellian velocity distributions and the "velocity filtration" mechanism (as first proposed by *Scudder* [1992a, 1992b] in a different context). The underlying principle is that the plasma is subjected to an attractive potential (in this case the centrifugal force due to corotation) and is not in thermodynamic equilibrium. The low-energy particles are confined in the potential well (which defines the centrifugal equator), whereas the more energetic particles can escape more easily. The farther out of the well, the larger the proportion of energetic particles and, hence, the higher the average kinetic energy. The temperature therefore increases with centrifugal latitude as the density decreases. This should be a general property of dilute planetary plasmaspheres and plasma tori (see *Meyer-Vernet* [2001] for a discussion at a basic level).

[6] We shall thus consider here charged particles confined by a corotating magnetic field $\boldsymbol{B}$ and examine the distribution as a function of position (curvilinear coordinate s along the magnetic field line with the origin located at the centrifugal equator; see Figure A1). Let $f_0(v)$ be the velocity distribution (which we assume in this section to be isotropic for simplicity) at $s = 0$, and suppose that the particles of mass m experience the force associated with an attractive potential ($\Phi(s) > 0$ with a minimum at $s = 0$). Liouville's theorem states that the velocity distribution is constant along a particle trajectory and, as a consequence, the velocity distribution at s is $f(s, v) = f_0(v_0)$. Conservation of energy requires that $v^2 = v_0^2 - 2\Phi/m$. One then finds that

$$f(s,v) = f_0\left(\sqrt{v^2 + 2\Phi(s)/m}\right), \tag{1}$$

assuming that s is accessible in phase space, as it is in this case of a monotonic and attractive potential. The moment of order q of the distribution at s along the field line is

$$M_q(s) = \int v^q f(s,v) d^3v = 4\pi \int_0^\infty v^{2+q} f_0\left(\sqrt{v^2 + 2\Phi(s)/m}\right) dv. \tag{2}$$

In general, f_0 is a decreasing function of velocity and, since the potential $\Phi(s)$ is monotonically increasing, the distribution $f_0\left(\sqrt{v^2 + 2\Phi(s)/m}\right)$ decreases with s. Consequently, all the moments decrease with s, in particular the density $n = M_0$.

[7] If f_0 is a single Maxwellian of temperature T, one can see from (1) that the distribution remains a Maxwellian for $s \neq 0$, and one can see from (2) that all the moments behave similarly with s. The temperature $T = mM_2/3k_BM_0$, where k_B is the Boltzmann's constant, or the effective temperature $T_{eff} = mM_0/k_BM_{-2}$ (which was obtained by a spectroscopic analysis of Bernstein modes measured by Ulysses [*Moncuquet et al.*, 1995]) thus remain constant. This means that with a Maxwellian distribution at the centrifugal equator the potential filters all the particles in the same way. In contrast, if the distribution f_0 has a suprathermal tail, i.e., more energetic particles than a Maxwellian should have, the higher moments decrease less rapidly with s than does the zero-order moment, so that the temperature *increases* with s. This generic temperature inversion was first shown in a graphic way by *Scudder* [1992a] and was proved analytically for any linear combination of Maxwellians [*Meyer-Vernet et al.*, 1995].

2.2. Polytropic Law and Kappa Velocity Distributions

[8] Let us first consider the simple case treated by *Meyer-Vernet et al.* [1995], which we will generalize in this paper, of the following (normalized) κ distribution

$$f_0(v) = \frac{\Gamma(\kappa+1)}{\pi^{3/2}\kappa^{3/2}\Gamma(\kappa-1/2)} \frac{n}{\Theta^3} \left[1 + \frac{v^2}{\kappa\Theta^2}\right]^{-\kappa-1}, \tag{3}$$

where Θ is the most probable speed, which we will denote the "thermal kappa speed," in an analogy to the thermal speed of a Maxwellian. Kappa distributions have been widely used to model space plasmas [*Vasyliunas*, 1968; *Collier and Hamilton*, 1995] and to approximate a Maxwellian at low

energies with a power law tail at higher energies (a nonthermal halo). Note that kappa distributions are typically found to have a κ index between 2 and 6 and that the distribution tends toward a Maxwellian when $\kappa \rightarrow \infty$. In this limit the two temperatures, T and T_{eff}, are equal, but for finite κ they have the different values $T = (m\Theta^2)/(2k_B)\kappa/(\kappa - 1.5)$ and $T_{eff} = (m\Theta^2)/(2k_B)\kappa/(\kappa - 0.5)$, though they both increase with latitude and obey the same polytropic law. To calculate the variation of these temperatures with position s along the magnetic field line, one inserts (3) in (1) and finds that the distribution remains a kappa function (with the same κ). Using moments calculation, one finds the density and temperature profiles to be

$$\frac{n(s)}{n(0)} = \left[1 + \frac{2\Phi(s)}{m\kappa\Theta^2}\right]^{\frac{1}{2}-\kappa} \tag{4}$$

$$\frac{T(s)}{T(0)} = \frac{T_{eff}(s)}{T_{eff(0)}} = \left[\frac{n(s)}{n(0)}\right]^{\frac{-1}{\kappa-1/2}}. \tag{5}$$

Thus, with such a κ distribution, the density and temperature follow a polytropic equation of state $T \propto n^{\gamma-1}$, where the polytropic index is less than one and related to κ via $\gamma = 1 - 1/(\kappa - 0.5)$ [*Meyer-Vernet et al.*, 1995].

[9] The polytropic law ($\gamma = 0.48$) observed in the IPT suggests that we should model the electrons in the torus with a κ distribution of $\kappa_\varepsilon \approx 2.4$. The measurements do not tell us however that the "true" electron velocity distribution is necessarily a kappa. Moreover, the value that we derive for the polytropic law comes from measurements made along the specific magnetic field line sampled by Ulysses (about $L = 8\ R_J$). The distribution on neighboring field lines does not necessarily have the same value of kappa or even maintain a kappa-like distribution.

2.3. Maxwellian Core and Halo Velocity Distributions

[10] The Voyager 1 electron measurements have been interpreted by *Sittler and Strobel* [1987] in terms of a superposition of two Maxwellian distributions with different temperatures and densities ("core and halo"). Such a distribution does lead to a temperature increase along the magnetic field as the density decreases.

[11] Let us take a function that is a sum of two Maxwellian distributions of densities n_c, n_h and temperatures T_c, T_h, corresponding to the core (cold) and halo (hot). With such a distribution, one can define the traditional temperature as $T = (n_cT_c + n_hT_h)/(n_c + n_h)$ and the effective temperature as $T_{eff} = (n_c + n_h)/(n_c/T_c + n_h/T_h)$. For simplicity, we will write $\alpha = n_h/n_c$ and $\tau = T_h/T_c$ (which implies $0 \leq \alpha < 1$ and $\tau > 1$). In this case, velocity filtration is especially simple to visualize since the density of the cold electrons n_c at the equator is multiplied by a factor $\beta(s) = \exp(-\Phi(s)/k_BT_c)$ at a distance s and is treated similarly for hot electrons. One obtains the variation in temperatures with latitude for such a core and halo distribution to be

$$T(s) = \frac{1 + \beta(s)^{\frac{1}{\tau}-1}\alpha\tau}{1 + \beta(s)^{\frac{1}{\tau}-1}\alpha} T_c \tag{6}$$

$$T_{eff}(s) = \frac{1 + \beta(s)^{\frac{1}{\tau}-1}\alpha}{1 + \beta(s)^{\frac{1}{\tau}-1}\alpha/\tau} T_c. \tag{7}$$

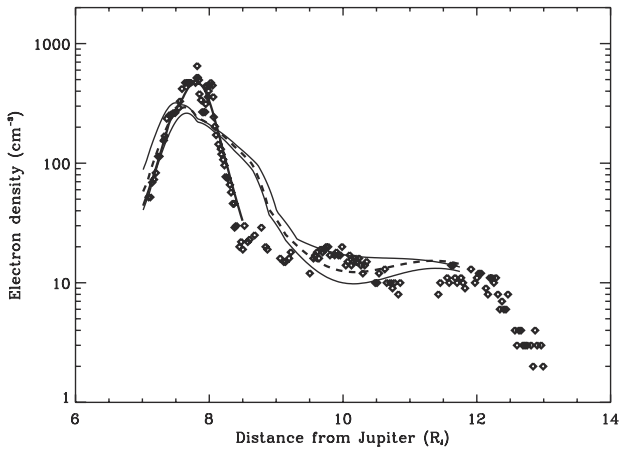

Figure 2. Electron density measurements from Ulysses (diamonds) compared to profiles extrapolated from Voyager 1 measurements. Two thin curves are the electron density profiles derived from the model of *Bagenal* [1994] using the O_6 magnetic field without current sheet and an isotropic velocity distribution (top curve) or with current sheet and anisotropy of 5 for the hot electrons (bottom curve). The dashed curve is a midrange model (O_6 + currentsheet + isotropy) [*NB*: the difference between O_4 and O_6 magnetic field models is small at these distances]. The thick curve, which is limited to the validity range of the polytropic law (i.e., $L \simeq 8\ R_J$) is the density profile deduced from the simplified kappa-like model of *Meyer-Vernet et al.* [1995].

[12] For Voyager 1, at the distance of $\sim 8\ R_J$, we have $\alpha \approx 0.02$ and $\tau \approx 12$, and if the conditions were the same for both Voyager 1 and Ulysses, (6) and (1) allow us to predict that a factor-of-4 variation in density should have produced a 50% variation in T and a 5% variation in T_{eff}. In reality, Ulysses measured a doubling of effective temperature for a factor 4 drop in n_c. The variation in T_{eff} is very small for a core and halo distribution because T_{eff} is close to T_c, which is constant along a field line since the core is Maxwellian.

3. A New Model of Latitudinal Structure for the IPT

3.1. Motivation

[13] It is clear that the strong latitudinal gradient in electron temperature, measured for the first time by Ulysses, requires a new model of the latitudinal structure of the torus. Figure 2 demonstrates the limitations of using the Voyager-based model [*Bagenal*, 1994] to model the densities measured by Ulysses in the region of the torus [*Hoang et al.*, 1993; *Moncuquet et al.*, 1997]. One can see that even with fairly extreme ion anisotropies and with a wide range in magnetic field models, the Voyager-based model cannot produce the tight confinement of plasma to the equator as observed by Ulysses, whereas *Meyer-Vernet et al.* [1995] were able to match the Ulysses electron data with a single kappa velocity distribution for a single ion species and electrons, although this model was admittedly oversimplified.

[14] With data obtained along spacecraft traversals through the torus that are widely separated in time, we

are still limited to 2-dimensional (2-D) models (where plasma properties vary with centrifugal latitude and radial distance but are assumed to be constant in the azimuthal direction). Moreover, it is quite possible that the properties of the torus have changed between the Voyager 1 flyby in 1979 and the Ulysses traversal in 1992. Remote sensing observations show that the torus density and temperature vary on timescales of days to years [*Thomas*, 1993]. Nevertheless, the purpose of this paper is to explore whether a single 2-D model of plasma distribution (uniform in longitude), where the number of adjustable parameters is kept to a minimum, is able to match the density profiles observed at very different times and to reproduce the observed variations in temperature with latitude.

3.2. Basics of the Model

[15] In discussing the notion of the centrifugal equator, we mentioned the component of the centrifugal force (due to the corotation of the plasma) that is parallel to the magnetic field. This force is proportional to the mass of the particle species considered and is consequently determined by the motion of the ions. From a microscopic view, in order for the plasma to remain neutral, the electrons must suffer an appropriate electromotive force to "follow" the motion of the ions. This force is produced by an ambipolar electric field $\boldsymbol{E}$ parallel to the magnetic field. This ambipolar electric field changes sign at the centrifugal equator and is derived from a negative electrostatic potential (denoted by ϕ_E) in order to confine negative charges. To first approximation, the corresponding potential energy $\Phi_e = -e\phi_E$ confines the electrons about the centrifugal equator to the same extent that the ions are confined by the combination of the centrifugal potential and the electric potential energy $Z_i e\phi_E$ (where Z_i designates the charge state of the ion).

[16] One can see that the potential Φ_e, needed to calculate the electron profile, depends fundamentally on the ions (via the equation for plasma neutrality) and on their velocity distributions as well as their chemical composition (see (A1) and (A2)). Since we only have electron measurements from Ulysses, we need to look elsewhere for information about the ions. Unfortunately, the separate velocity distributions of the ion species in the torus (S^+, S^{++}, S^{+++}, O^+, O^{++}, H^+, Na^+, and SO_2^+) are not well determined by the Voyager plasma science (PLS) instrument in the outer, warm region of the IPT. However, there is strong evidence that both the electron and ion distributions are non-Maxwellian [*Bagenal and Sullivan*, 1981; *Sittler and Strobel*, 1987]. Furthermore, the mean free path of the ions (which are $\sim$10 times hotter than the electrons) is also much larger than that of the electrons, which argues for a still less effective thermalization for the ions [*Smith and Strobel*, 1985]. Thus there is every reason to suppose that the ions are not in local thermal equilibrium, just as the Ulysses data showed that the electrons are not thermalized.

[17] In their analytical model describing the velocity distribution of the ions with a kappa function, *Meyer-Vernet et al.* [1995] made the simplifying assumption of a single ion species having a similar (isotropic) distribution to the electrons, which is certainly not justified, as they frankly admit. This limitation can be overcome by calculating separate density profiles using a set of equations (equation (4)), with a potential energy $\Phi_e = -e\phi_E$ for the electrons and $\Phi_i = Z_i e\phi_E + \phi_C$ for each ion species of charge $Z_i e$ (where ϕ_C is the centrifugal potential; see (A2). This involves a set of nine equations (one for electrons and eight for the ion species listed above) with 10 unknowns (the densities and the ambipolar electrostatic potential ϕ_E), which is closed by the equation of charge neutrality $\Sigma_i n_i Z_i = n_e$.

3.3. Anisotropic Bi-Kappa Ion Distributions

[18] When dealing with nonthermal velocity distributions for the ion species, we must consider the issue of their thermal anisotropy, i.e., the difference in temperature parallel and perpendicular to the magnetic field and the concomitant magnetic mirror force. Unfortunately, the Voyager PLS instrument was only able to measure the perpendicular temperature of the ions. The results reported by *Bagenal* [1994] were consistent with a perpendicular velocity distribution of the ions having a thermal core with a nonthermal "tail" or "halo." The Galileo plasma instrument has a full angular response and indicated that the thermal core of the ion distribution is isotropic [*Crary et al.*, 1998]. In contrast, there is good reason to believe that the halo component of the ion distribution should be highly anisotropic. When neutral atoms (escaped from Io's atmosphere) are first ionized, they experience Jupiter's strong magnetic field and "pickup" a gyro-motion perpendicular to the magnetic field equal to the bulk (corotation) speed of the plasma. The initial parallel motion of the pickup ions is small. Hence we might expect that a population of freshly ionized particles would have a highly anisotropic distribution. Eventually, one expects these pickup ions to be partially thermalized by plasma waves and, on longer timescales, by collisions. While the timescales for partial thermalization of such a "ring" distribution are not well known, it is clear that we should expect a substantial anisotropic suprathermal component for the ion velocity distribution.

[19] For the purposes of modeling an anisotropic distribution having a suprathermal tail, we adapt an anisotropic kappa distribution from *Summers and Thorne* [1992], which we call bi-kappa (by analogy to bi-Maxwellians) and is of the form

$$f_0(v_\parallel, v_\perp) = \frac{\Gamma(\kappa+1)}{\pi^{3/2}\kappa^{3/2}(\kappa-1/2)}\frac{n}{\Theta_\parallel\Theta_\perp^2}\left[1+\frac{v_\parallel^2}{\kappa\Theta_\parallel^2}+\frac{v_\perp^2}{\kappa\Theta_\perp^2}\right]^{-\kappa-1}. \tag{8}$$

[20] Applying Liouville's theorem with the conservation of energy and magnetic moment ($\mu \propto v_\perp^2/B$), as in the isotropic case, one derives the density distribution for each particle species. Recall that Liouville's theorem allows one to express the distribution as a function of the curvilinear coordinate s along the magnetic field, in the presence of a monotonic attractive potential $\Phi(s)$, as

$$f(s, v, v_\perp^2) = f_0\left(\sqrt{v^2 + 2\frac{\Phi(s)}{m}}, v_\perp^2\frac{B(0)}{B(s)}\right). \tag{9}$$

[21] By expressing the thermal anisotropy at the equator as $A_0 = \Theta_\perp^2/\Theta_\parallel^2 = T_\perp(0)/T_\parallel(0)$, we can use (9) to calculate the

moments of the distributions to derive the latitudinal profiles of density and temperature as follows:

$$\frac{n(s)}{n(0)} = \left[1 + \frac{2\Phi(s)}{m\kappa\Theta_{\parallel}^2}\right]^{\frac{1}{2}-\kappa} \frac{1}{A_0 + (1-A_0)\frac{B(0)}{B(s)}}, \quad (10)$$

$$\frac{T_{\parallel}(s)}{T_{\parallel}(0)} = \left[1 + \frac{2\Phi(s)}{m\kappa\Theta_{\parallel}^2}\right], \quad (11)$$

$$\frac{T_{\perp}(s)}{T_{\perp}(0)} = \left[1 + \frac{2\Phi(s)}{m\kappa\Theta_{\parallel}^2}\right] \frac{1}{A_0 + (1-A_0)\frac{B(0)}{B(s)}}. \quad (12)$$

[22] When $\kappa \rightarrow \infty$, one retrieves the results obtained with a bi-Maxwellian distribution of *Huang and Birmingham* [1992]. In this case, we get, from (12) with $A_0 > 1$ (as expected in the torus; see the above discussion), a perpendicular temperature which decreases with latitude and, from (11), a constant parallel temperature. When $A_0 = 1$ (isotropy), one retrieves the density profile (equation (4)) found by *Meyer-Vernet et al.* [1995].

[23] Note that with these bi-kappa distributions, neither the parallel nor the perpendicular temperature strictly follow a polytropic law. The parallel temperature increases with latitude independently of B, while the perpendicular temperature has an additional variation along the magnetic field due to the change in field strength. This means that the anisotropy is not constant along magnetic field lines, but decreases if $A_0 > 1$. Since the change in magnetic field strength is small (<20% over the latitudinal range of Ulysses), this is a minor effect, unless the anisotropy at the equator is particularly strong.

[24] To illustrate the relative effects of the anisotropy and of the suprathermal tail, we show in Figure 3 several latitudinal density profiles calculated with different values of the parameters A_0 and κ. We chose a longitude (201°) where the magnetic and rotational equators are separated by the maximum amount (9.6°) to illustrate the limited influence of the changing magnetic field strength on the density distribution. The density maximum is located at the centrifugal equator (at a magnetic latitude of 9.6/3 = 3.2°), and the net effect of the magnetic mirror force is a small asymmetry about the centrifugal equator.

[25] The profiles in Figure 3 were obtained by solving (10) for both the electrons and a single ion species with the equation of charge neutrality $n_e(s)/n_e(0) = n_i(s)/n_i(0)$, which permits the elimination of the electric potential ϕ_E. One can see that the kappa distributions have the tendency to tightly confine the particles to the equator while allowing a substantial population at high latitudes. The effect of increasing the thermal anisotropy ($A_0 = 1-3$), for either the Maxwellian or kappa cases, is to further confine the plasma to the equator.

[26] With these tools in hand, including the flexibility of varying the unknown parameters A_0 and κ, we are now able to model the density distributions observed by different spacecraft as they traversed the torus.

4. Building a 2-D Model for the IPT

[27] To construct a 2-D model of the density and temperature in the torus, the nine different particle species yield

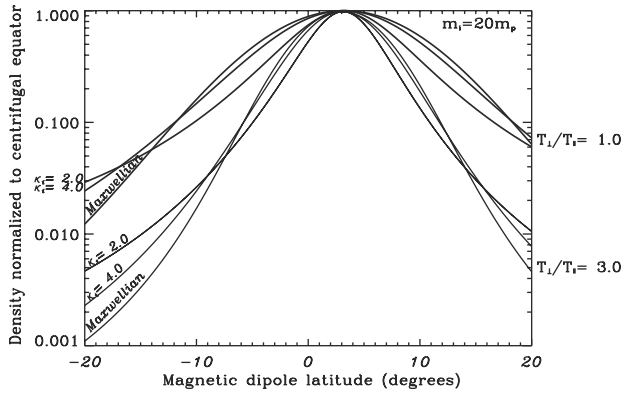

Figure 3. Plasma density (normalized to the centrifugal equator), as a function of the magnetic latitude (Jovian tilted dipole model), for two kappa values (2 and 4) of the velocity distribution of a typical ion of the Io torus ($m_i = 20\ m_p$, $Z_i = +1$) and compared to the density profile obtained with a Maxwellian distribution ($\kappa_i \rightarrow \infty$). Bold curves are isotropic distributions and thin curves have a temperature anisotropy $T_{\perp}/T_{\parallel} = 3$ (note that in all cases, the kappa of the electrons was set to 2.4 [*Meyer-Vernet et al.*, 1995] and their anisotropy was set to 1.2 [*Sittler and Strobel*, 1987]).

nine equations of the form (10) which, completed with the equation of charge neutrality, permit us to calculate the normalized density profiles along the magnetic field $n(s)/n(0)$. The normalized temperature profiles $T_{\parallel,\perp}(s)/T_{\parallel,\perp}(0)$ are then obtained using the nine corresponding equations of the form (11) or (12). Details of the calculation are given in Appendix A.

[28] Since the model has two dimensions, we may distinguish between input parameters concerning the radial dependency (namely, the equatorial density $n(0)$ and temperatures $T_{\parallel,\perp}(0)$ at a given Jovicentric distance) and those concerning the latitudinal dependency of the model (namely $n(s)$ and $T_{\parallel,\perp}(s)$ at an altitude s from the centrifugal equator), which both depend on the magnetic field geometry and on the bi-kappa distribution parameters A_0 and κ.

4.1. Input Parameters

[29] Considering first the radial dependency of the model, we have the following input parameters: the densities of each species at a reference point (e.g., the location of the spacecraft at the time of in situ measurements, the densities $n(0)$ at the centrifugal equator being then extrapolated using (10)) and the values of the parallel and perpendicular temperatures $T_{\parallel}(0)$ and $T_{\perp}(0)$ at the centrifugal equator (or, equivalently, the parallel thermal speed $\Theta_{\parallel}$ and the thermal anisotropy at the equator A_0). In this paper the input densities and temperatures are those used by *Bagenal* [1994], comprising 48 points between 4 and 12 R_J based on the inbound Voyager 1 plasma measurements and the Voyager ultraviolet spectrometer (UVS) emissions. The radial profiles along the spacecraft trajectory (illustrated in Figure 1) are shown in Figure 4 and constitute the "reference data set" for the radial structure of the IPT.

[30] In addition, since the latitudinal changes in density (equation (10)) as well as in temperature (equations (11) and (12)) are given along the magnetic field lines, their

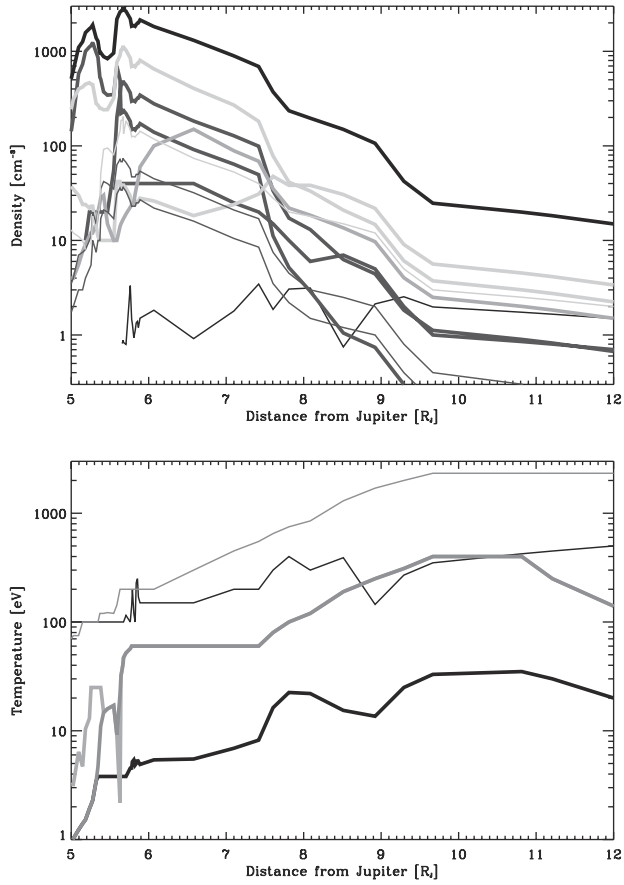

Figure 4. (top) Reference densities and (bottom) temperatures of the main particle species (from Voyager 1) used to compute our torus model (identical to *Bagenal* [1994]). The electron parameters are plotted in black, the densities of sulfur ions ($S^{+,\ ++,\ +++}$) are in red, and the densities of oxygen ions ($O^{+,\ ++}$) are in blue; the proton densities are plotted in green. The parameters of cold species (core) are plotted as bold lines and the parameters of hot species (halo) are plotted as thin lines (there is no halo for minor species S^{+++}, O^{++}, and protons). The core and halo temperatures (pink) are the same for all ions (except for the protons between 5 and 6 R_J, which are green). See color version of this figure at back of this issue.

calculations require a reliable model of the Jupiter magnetic field and, eventually, of the azimuthal current sheet. At first approximation the Jupiter magnetic field is assumed to be a tilted dipole (sketched in Appendix A) to which we may add, as did *Bagenal* [1994], nondipolar contributions from the Goddard Space Flight Center (GSFC) O_4 or O_6 models, with or without current sheet contributions [*Connerney*, 1992]. Note also, that we have simply assumed, to express the centrifugal potential in (A2), that all the torus plasmas rigidly corotate with Jupiter, while the bulk plasma speed is indeed slower than the exact corotation speed in the outer IPT [*Hill*, 1980; *Belcher*, 1983], as recently confirmed with Galileo plasma measurements [*Frank and Paterson*, 2000]. But the consequences to our model of this centrifugal speed variation with radial distance are actually negligible, especially when compared to those due to possible variations of the main unknown inputs of the model, namely, the ions' kappa and anisotropy values, which we discuss now.

[31] The choices of kappa and of the anisotropy parameters for the ion species are not well constrained by the observations. Nevertheless, we can eliminate the most extreme values. First of all, the Voyager 1 observations of a nonthermal tail in the ion velocity distributions indicate that the kappa must be finite ($\lesssim$10). We can also eliminate values $A_{0i} \gtrsim 10$. Although such an anisotropy matches the equatorial confinement observed by Ulysses, the assumption of high anisotropy requires a strong increase in equatorial temperature with radial distance, which conflicts with remote sensing observations and with the plasma cooling on expansion.

[32] Unfortunately, the data do not sufficiently constrain the ion temperature anisotropy A_{0i} and the ion kappa values κ_i. Indeed, among the four in situ data sets available to us, only two can constrain these parameters, namely the electron density at Ulysses (whose confinement requires a significant anisotropy) and the temperature increase with radial distance at Voyager 1 (which is not compatible with such a significant anisotropy if the distributions are Maxwellian). To derive some more precise constraints on A_{0i} and κ_i, we would need either a simultaneous measurement of the temperature at the equator for Voyager 1 or a measurement of the ion temperature at Ulysses (along the magnetic field), neither of which was obtained. Therefore, the most conservative constraint we can derive is that A_{0i} is >1, probably <5, that κ_i is finite, probably <6.

[33] In this paper we have chosen values for the ion distributions of $\kappa_i = 2$ and $A_{0i} = 3$ as a compromise that (1) matches the confinement of the plasma to the centrifugal equator observed by Ulysses, (2) produces a relatively flat (to decreasing) variation of temperature with radial distance (consistent with expectations of plasma cooling by expansion), (3) is consistent with the increase of temperatures with latitude observed by Voyager 1 beyond 8 R_J, and, finally, (4) gives an increase in ion temperature with latitude comparable to that observed for the electrons on Ulysses. We discuss the first three issues in more detail in section 4.2.

4.2. Matching the Model with In Situ Measurements

4.2.1. Electron Density from the IPT Passes

[34] In Figure 5 we show the comparison of electron densities measured by Voyager 1, Voyager 2, Ulysses and Galileo with the predictions at the spacecraft locations from the (1) Maxwellian isotropic, (2) near-isotropic bi-kappa model ($\kappa_i = 2$, $A_0 = 1.2$ for all species), or (3) anisotropic bi-kappa model ($\kappa_i = 2$, $A_{0i} = 3$) based on Voyager 1 inbound plasma conditions (referenced hereinafter as case 1, 2, or 3). The match of the model to data obtained in March 1979, July 1979, and February 1992 is remarkable considering we are using an azimuthally symmetric model with a single value of kappa for all ions and that the values of kappa and anisotropy are assumed to be constant throughout the torus.

[35] To match the Ulysses measurements, we had to enhance the total charge density throughout the torus by a factor of 1.9 compared with the Voyager epoch. This enhancement is comparable to the higher overall densities measured by Galileo in 1995 [*Frank et al.*, 1996; *Gurnett et*

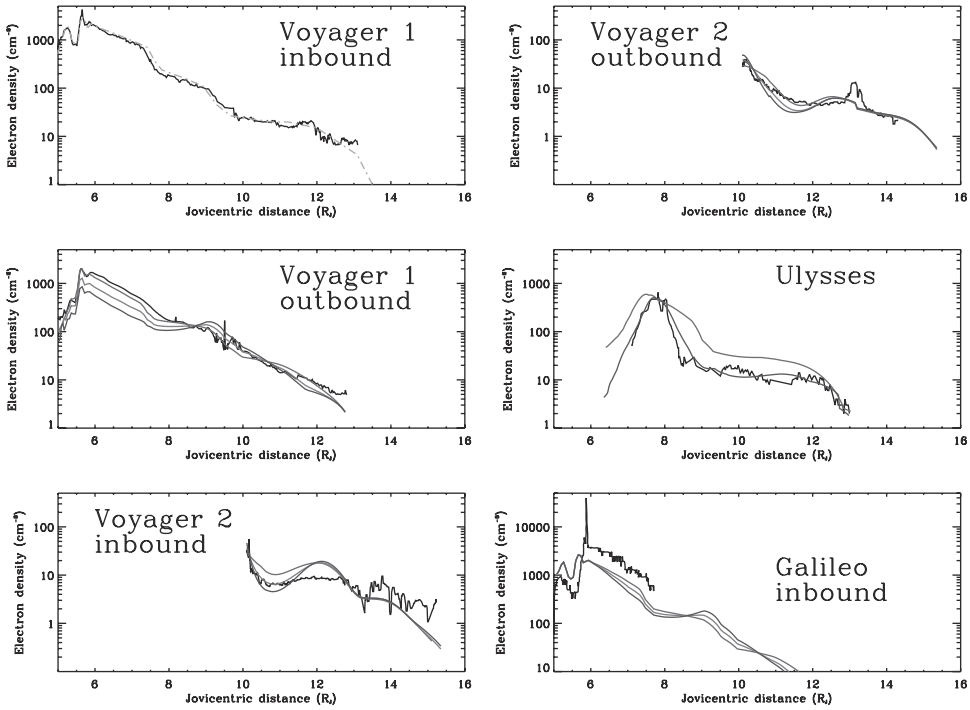

Figure 5. Comparison of computed models (colored lines) with measurements (black lines) of electron density from Voyager 1 and 2, Ulysses, and Galileo. The Voyager 1 inbound density profile is shown only with the reference data set (dash-dotted green line), which is used for building the other profiles. The predicted profiles have been superposed on the data: blue for the Maxwellian isotropic model; orange for the bi-kappa model with $\kappa_i = 2$, $\kappa_e = 2.4$, $A_{0i} = A_{0e} = 1.2$; and red for the bi-kappa model with $A_{0i} = 3$ and all other parameters as above. (Note that for Ulysses the density profiles have been multiplied by 1.9. The log-vertical (density) ranges are not the same for all panels.) See color version of this figure at back of this issue.

al., 1996; *Bagenal et al.*, 1997]. The Ulysses measurement of the tight confinement of the density to the equator (illustrated by the narrow peak around 8 R_J) could not be matched by using an isotropic kappa, nor by a highly anisotropic ($A > 10$) bi-Maxwellian. On the other hand, after selecting a normalization factor (1.9) and values of κ and A_0 to match the equatorial confinement, the densities were also very well matched beyond 9 R_J when Ulysses was at high latitudes. The model/data root-mean-square (RMS) is ~60% for case (3) and 270% for case (1).

[36] When comparing the model (based on Voyager 1 inbound conditions) with the densities measured on the Voyager 1 outbound passage, we see that the densities beyond 9 R_J match very well, but in the main part of the torus the observed densities are about a factor of 3 higher than predicted by the anisotropic ($A = 3$) bi-kappa model. Since the latitudinal ranges of the inbound and outbound passes are similar, this substantial difference in density level suggests a strong longitudinal asymmetry in the torus. This asymmetry had already been noted by *Hoang et al.* [1993] from comparison with previous models. When we compare the longitude of the spacecraft with longitudinal variations in emission intensity observed by *Schneider and Trauger* [1995], however, we find that the ground-based emissions predict the opposite of what was observed (namely, that the outbound densities should have been lower rather than higher than those based on the inbound observations). Of course, this might also suggest that the temperature anisotropy is not constant throughout the torus but instead is weaker between 6 and 9 R_J than beyond. It is also worth noting that the isotropic Maxwellian provides a significantly better fit in this region than either of the kappa distributions, with a model/data RMS of ~17%, against 26% for case (2) and 36% for case (3).

[37] When comparing the model with the Voyager 2 data [from *Belcher*, 1983, Figure 3.14], obtained 6 months after Voyager 1, we find that the bi-kappa model, without any normalization factor, matches the densities at closest approach to Jupiter that occurred close to the equator at ~10 R_J. The model/data RMS are: on inbound, for case 1, 68%; case 2, 48%; and case 3, 56%; and on outbound, for case 1, 29%; case 2, 25%; and case 3, 34%. More precisely, a quasiisotropic ($A = 1.2$) kappa model ($\kappa = 2$) yields the correct density gradient when the spacecraft comes (inbound as well as outbound) from the centrifugal equator up to higher latitudes (with a maximum at ~13°S) at a Jovincentric distance of ~11 R_J (see Figure 1). On the inbound trajectory, however, when the spacecraft is close to the equator again, say around 12 R_J, the model overpredicts the observations by about a factor of 2. In contrast, the model underpredicts the observations by about the same factor beyond 13 R_J, when the spacecraft returned to high latitudes. This difference might be explained by the plasma being hotter (and thus spread farther from the equator) at the time of Voyager 2. A hotter plasma at the time of Voyager 2 is consistent with higher

electron temperatures inferred from UV emissions by *Sandel et al.* [1979]. On the other hand, the differences might also be due to distortions in the magnetic field by a change in the equatorial current sheet, which can be significant beyond 10 R_J.

[38] We have also shown in Figure 5 the electron density profile [from *Bagenal et al.*, 1997] measured by Galileo during its pass through the torus on 7 December 1995. In the outer part of the IPT the electron density observed by Galileo is roughly a factor of 2 higher than the Voyager 1 value and thus about the same as the equatorial density inferred from Ulysses observations. Unfortunately, data are available only inward for <8 R_J and, because the Galileo inbound trajectory was very close to the centrifugal equator at these distances (see Figure 1), these data cannot be used to constrain our model. Let us remark, however, that the slope of the decreasing density with distance is better predicted with a near-isotropic kappa model (i.e., $A_0 = 1.2$ and $\kappa_i = 2$) than with a Maxwellian core and halo or with a higher anisotropy. It is also worth noting that all models fail to predict the magnitude of the ledge observed by Galileo near 5.8 R_J, even ignoring the spike associated with the close approach to Io.

4.2.2. Equatorial Profiles

[39] Figure 6 shows the plasma parameters at the centrifugal equator extrapolated from data measured along the spacecraft trajectory using (10) and (12), with $\kappa = 2$ and $A_0 = 3$ for the ions and with $\kappa_e = 2.4$ (measured by Ulysses) and $A_{0e} = 1.2$ [after *Sittler and Strobel*, 1987] for the electrons. These radial profiles along the centrifugal equator derived using our bi-kappa model are significantly different from those obtained by *Bagenal*, [1994, Figures 5 and 6] at radial distances >8 R_J where the Voyager 1 spacecraft was well below the centrifugal equator. Indeed, because the bi-kappa distribution produces a stronger confinement of the plasma to the centrifugal equator than Maxwellian distributions, the equatorial densities are substantially enhanced beyond 8 R_J.

[40] The flatter radial profile of density has important implications for the radial diffusion of plasma in the torus [*Siscoe and Summers*, 1981]. Of even greater significance, perhaps, is the difference in radial temperature profiles produced by the two models illustrated by the bottom panels of Figures 4 and 6.

4.2.3. Variation in Temperature Measured by Voyager 1

[41] First of all, we should clarify that the temperatures in Figure 6 are the usual perpendicular temperatures, i.e., defined from the moments of order 2 of the anisotropic bi-kappa distribution and extrapolated to the centrifugal equator by (12). We plot the perpendicular temperatures because we wish to compare them with the temperatures measured by Voyager 1. For easier comparison, since these perpendicular temperatures at Voyager 1 were provided as distinct core and halo temperatures (see Figure 4), we have thus plotted (dotted line) in Figure 6 a total (core and halo) temperature of these in situ measurements (this temperature can be interpreted also as the total equatorial temperature in the absence of the velocity filtration effect).

[42] On examining the radial profiles of temperatures extrapolated to the centrifugal equator with the bi-kappa model (Figure 6) with those measured at the location of Voyager 1, there are substantial differences. On one hand, since the temperatures were poorly determined by the Voyager plasma instrument, all the ionic species were assumed to have the same temperature. However, when the temperatures are extrapolated to the equator by using our model under this last assumption, we find straightforwardly from (12) and (A5) that the temperatures of the different ion species will be different at the centrifugal equator, the sulfur (heavier) ions being colder than the oxygen ions for the same charge state. However, this result is mainly a consequence of the lack of discriminating temperature data at Voyager, and so we will not discuss it further. On the other hand, because of velocity filtration the equatorial temperatures are lower than those measured off the equator. This is particularly noticeable beyond 8 R_J where Voyager 1 dipped more that 1 R_J below the equator (see Figure 1). The net result is that the equatorial temperature profile is much flatter than the radial profile measured at the spacecraft, where the temperature was observed to

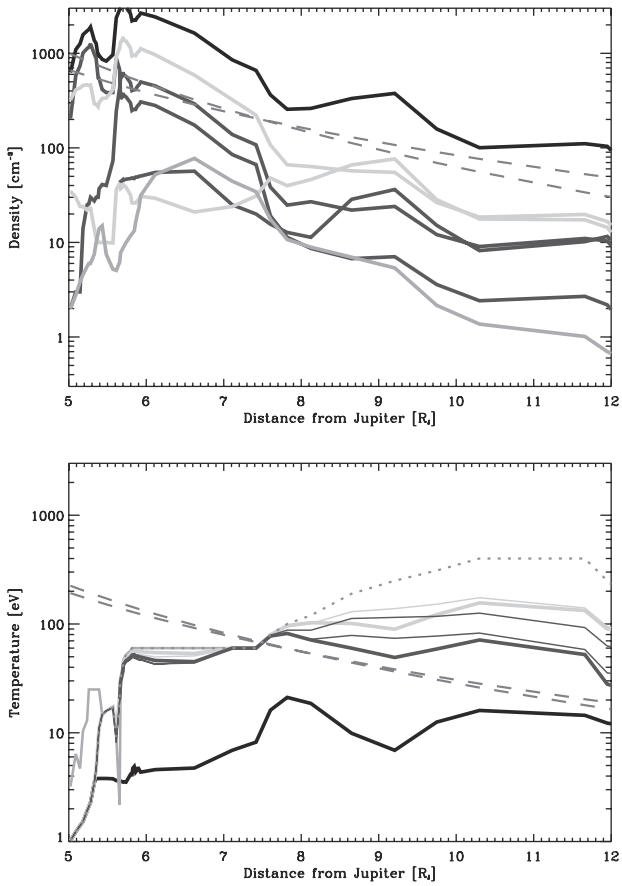

Figure 6. (top) Total densities and (bottom) perpendicular temperatures extrapolated from Voyager 1 to the centrifugal equator, using a bi-kappa function velocity distribution for the particles ($\kappa \equiv 2$ and $A_0 \equiv 3$ for *all* the ions; $\kappa_e = 2.4$ and $A_{0e} = 1.2$ for the electrons). Electrons are in black, sulfur is in red, oxygen is in blue, and protons are in green. We have superposed the former core plus halo ion temperature (pink dotted line) and adiabatic gradients (orange dashed lines) decreasing as L^{-4} or as L^{-3} for the densities and as $L^{-8/3}$ or as L^{-3} for the temperatures. See color version of this figure at back of this issue.

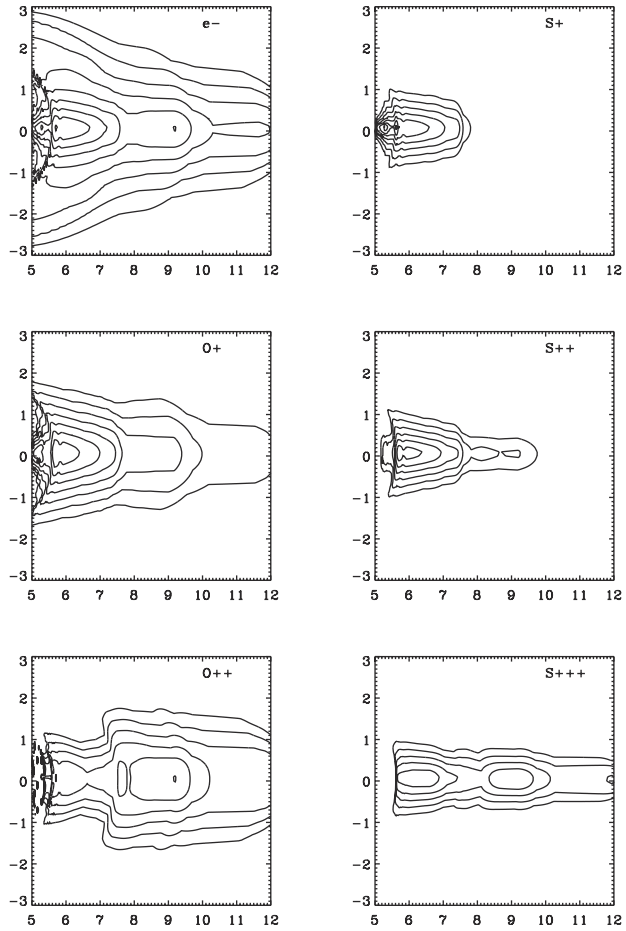

Figure 7. Contours of particle density in the meridian plane for International Astronomical Union (IAU) System III longitude of 292°. The x axis gives distance from Jupiter (R_J), the y axis gives centrifugal altitude (R_J), $\kappa_i = 2$, $A_{0i} = 3$, $\kappa_e = 2.4$ and $A_{0e} = 1.2$. All contour levels are spaced by a factor of 2. The electron contours decrease from 3200 cm^{-3}. The contours for O^+, S^+, and S^{++} decrease from 1600 cm^{-3}, and the contours for O^{++} and S^{+++} decrease from 80 cm^{-3}.

increase substantially with radial distance. Otherwise stated, and as was first pointed out by *Moncuquet* [1995], a substantial part of the ion temperature increase measured by Voyager 1 beyond 8 R_J can be ascribed to the increasing centrifugal latitude of the spacecraft. This result was confirmed by *Thomas and Lichtenberg* [1997], who interpreted their ground-based spectroscopic IPT observations at 6 R_J, showing a significant increase in perpendicular ion temperature with distance from centrifugal equator, by using the simplified "kappa model" of *Meyer-Vernet et al.* [1995].

[43] One would expect the plasma to cool on expansion as it diffuses radially outward from Io. The power laws shown in Figure 6 illustrate what one would expect for isotropic adiabatic expansion, i.e., $n \propto L^{-4}$ and $T \propto L^{-8/3}$ [*Herbert and Sandel*, 1995], or, because we assume here a substantial ion temperature anisotropy, for adiabatic expansion under conservation of the first adiabatic invariant, i.e., $T_\perp \propto L^{-3}$ (and a total density charge which may decrease also as L^{-3} if we assume a constant centrifugal scale height). Thus our model yields an equatorial temperature profile until ~9.3 R_J (about the Europa orbit), which may be roughly interpreted as the adiabatic cooling of a plasma in radial diffusion, while there is still a "missing" heating source beyond this distance in order to fully explain the Voyager 1 PLS temperature data. Our model is also more consistent with UV spectra observations at Voyager 1 and with ground-based observations [*Herbert and Sandel*, 1995; *Thomas*, 1995]. Indeed, the vertical distribution of emissions from the torus suggest a decrease in temperature with distance. Note that the temperature anisotropy works in the opposite direction; the perpendicular temperature is greater at the equator when there is significant anisotropy (from (12) or from *Huang and Birmingham* [1992] for the bi-Maxwellian case).

4.3. Density and Temperature Isocontours

[44] To illustrate our new 2-D model of the IPT and the effect of choosing values of $\kappa_i = 2$ and $A_{0i} = 3$, we present contours of plasma density in Figure 7. The torus densities are presented in the meridian plane for a longitude of 292° (where the magnetic and centrifugal equators coincide). In order to allow direct comparison with *Bagenal*, [1994, Figure 8], we have used the O_4 with the current sheet magnetic field model. Apart from the differences at the centrifugal equator already discussed, the most notable difference is that the plasma is more tightly confined to the equator at distances beyond ~8 R_J producing the appearance more of a plasma sheet rather than the sharp outer boundary of a torus.

[45] In Figure 8 we have also plotted the contours of proton density. It is worth noting that the inputs density and temperature for protons (green lines in Figure 4) are very badly known, especially because protons have dropped below the energy threshold of the PLS detector [*Bagenal*, 1994], and so the proton density we obtain at the equator (green line in top panel of Figure 6) has a bad reliability (it is however compatible with an upper limit of 60 cm^{-3}

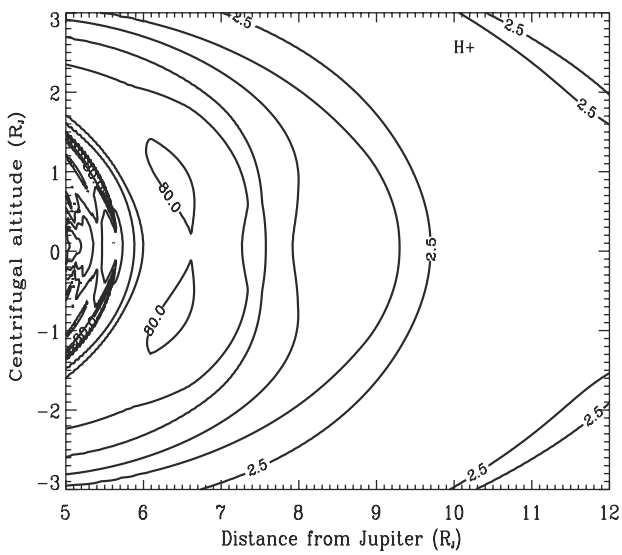

Figure 8. Contours of proton density in the meridian plane for IAU System III longitude of 292°, with $\kappa_i = 2$, $A_{0i} = 3$, $\kappa_e = 2.4$, and $A_{0e} = 1.2$. The contour levels are spaced by a factor of 2.

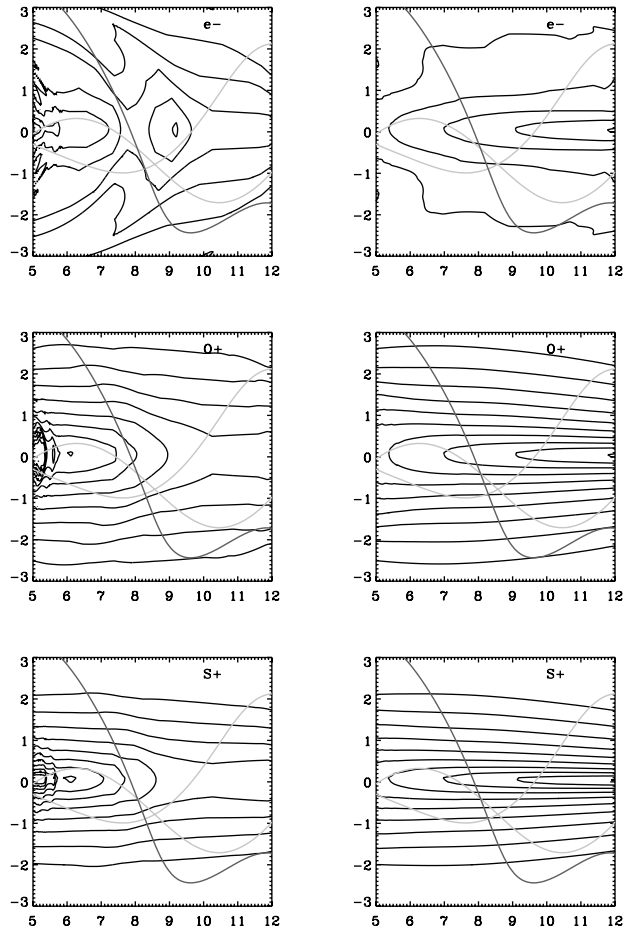

Figure 9. (left) Contours of temperature for electrons (e^-), S^+, and O^+ in the meridian plane for IAU System III longitude of 292°. The x axis gives distance from Jupiter (R_J), the y axis gives centrifugal altitude (R_J), $\kappa_i = 2$, $A_{0i} = 3$, $\kappa_e = 2.4$, and $A_{0e} = 1.2$. All contour levels are spaced by a factor of 2. The electron contours increase from 1 eV. The ions contours increase from 10 eV. (right) Temperature contours assuming an adiabatic L dependence at the centrifugal equator of L^{-3} (orange line in Figure 6). Colored curves are the trajectories of Ulysses (red) and of Voyager 1 (green). See color version of this figure at back of this issue.

derived from whistler wave analysis [*Crary et al.*, 1996]). Nevertheless, we may observe that the maximum proton density is offset from the centrifugal equator (by ∼8° centrifugal latitude). As noted in section 3.2, the latitudinal structure of the Io torus depends fundamentally on the heavier ions (oxygen and sulfur), which dominate the composition and which more strongly experience the confining centrifugal force than the protons. This results in a rather high electrostatic potential Φ_e (see Figure A2) in order to confine the electrons similarly to the heavy ions so as to preserve the plasma neutrality. The consequence for the protons is that the confining centrifugal force is weaker at the equator than the electrostatic force, and this tends to spread them out of the centrifugal equator.

[46] Figure 9 (left-hand column) presents isocontours of temperature for electrons, S^+ and O^+. The temperature has a minimum at the equator and increases (due to velocity filtration) with latitude. Notice that the latitudinal temperature gradients are stronger for the heavier (sulfur) species than for the oxygen species. In Figure 9 (right-hand column) we have also plotted the temperature contours obtained assuming that the equatorial temperature decreases adiabatically with radial distance (L^{-3}). The spacecraft trajectories of Voyager 1 (green) and Ulysses (red) have been superposed to illustrate how one would expect a temperature increase to be observed by Ulysses on its roughly north-to-south trajectory and by Voyager 1 beyond 7 R_J, while the equatorial temperature is assumed to decrease with distance from Jupiter.

5. Summary and Final Remarks

[47] With a kinetic collisionless model assuming bi-kappa velocity distributions for ions and electrons, we have been able to model various aspects of the Ulysses data: the tight confinement of the plasma to the equator and the variation in electron temperature with latitude. Using input parameters based on Voyager 1 conditions [*Bagenal*, 1994] enables us to model many features of the density measurements made by Voyager 1, Voyager 2, Ulysses, and Galileo. Differences between the model and the observations suggest variations in density of about a factor of 2 with longitude (for Voyager 1 inbound data) or with time (between Voyager, Ulysses, and Galileo epochs).

[48] The bi-kappa distribution also enables us to explain part of the increase in ion temperature observed by Voyager 1 between 7 and 10 R_J where the spacecraft was ∼1 R_J below the centrifugal equator. When the ion temperatures are extrapolated to the equator with the bi-kappa model, we find that the temperature increases less rapidly with radial distance (compared to the earlier core-halo fit), which is more nearly consistent with both the plasma cooling quasiadiabatically as it diffuses radially outwards and with observations of the vertical distribution of emissions from the torus diminishing with radial distance from Jupiter [*Herbert and Sandel*, 1995; *Thomas*, 1995].

[49] It is noteworthy that the choice of the bi-kappa distribution parameters which enable us to obtain the above results, namely, the ion anisotropy $A_{0i} = 3$ and the ion kappa value $\kappa_i = 2$, is a working compromise and not the result of any fitting-to-data process. We cannot indeed

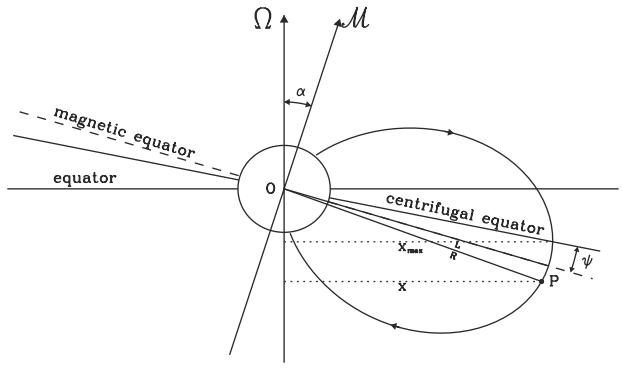

Figure A1. Geometry of a tilted dipole field.

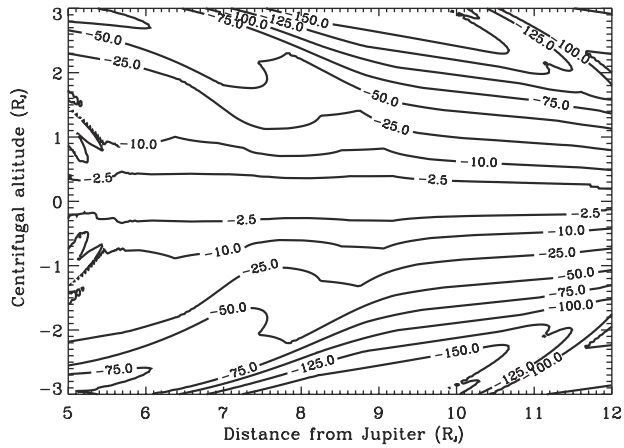

Figure A2. Contours sample, in a meridian plane, of the ambipolar electric potential ϕ_E (labeled in volts).

derive precise values of these parameters, since we lack ion measurements over a significant latitude range. The best constraint we can derive is $1 < A_{0i} < 5$ and κ_i sufficiently moderate so that the bi-kappa is not equivalent to a bi-Maxwellian (say, $\kappa_i < 6$ for all species in the outer IPT). We may, however, conclude that a kinetic collisionless model, using a non-Maxwellian anisotropic distribution, provides physical explanations for both the unexpected behavior of the temperature along the magnetic field lines as seen at Ulysses and the misunderstood behavior of the equatorial temperature with distance from Jupiter as seen at Voyager 1 [*Moncuquet*, 1997].

[50] From a basic plasma physics point of view, this illustrates an important consequence of the lack of collisions in space plasmas. The particles have non-Maxwellian velocity distributions, so that they cannot be adequately modeled by (multi-) fluid equations, but require instead a kinetic approach. The present results show that kinetic effects play an important role not only on small scales but also for describing largescale structures [*Meyer-Vernet*, 2001].

Appendix A: Geometrical and Numerical Method

[51] The geometry of a tilted dipole field is shown in Figure A1. The centrifugal equator is defined as the locus of the most distant points from the spin axis along magnetic field lines. The centrifugal equator is plotted here in the Jovian meridian plane, which contains the magnetic moment $\mathcal{M}$ of a centered dipole, tilted by α with respect to the Jupiter spin axis Ω. The angle ψ between the magnetic and centrifugal equator is maximum in this (Ω, $\mathcal{M}$) plane and is $\sim\alpha/3$ for small α [*Hill et al.*, 1974] (for Jupiter, ψ is $\sim 3.2°$). A given point P of the magnetosphere is defined by two coordinates: (1) the dipole equatorial radius L of its own magnetic field line and (2) its centrifugal latitude, that is, the angle between *O-P* and the centrifugal equator.

[52] In constructing a 2-D model of the spatial distribution of a plasma with N particle species, we need to determine the properties at each point P (described by the value of its curvilinear coordinate along the magnetic field) using a system of $N+1$ equations (the equations of density equation (10) plus charge neutrality) with $N + 1$ unknowns (the densities and the ambipolar electric potential ϕ_E at point P).

$$\sum_{\alpha}^{N} n_\alpha(s, \Phi_\alpha(s, \phi_E)) Z_\alpha = 0, \tag{A1}$$

where Φ_α is the energy potential at point P, the sum of centrifugal, gravitational, and electrostatic potential energies

$$\Phi_\alpha(s, \phi_E) = \frac{m_\alpha \Omega_J^2}{2}\left(x_{\max}^2 - x^2\right) + m_\alpha GM_J\left(\frac{1}{r} - \frac{1}{r_0}\right) + Z_\alpha e\phi_E, \tag{A2}$$

where Ω_J is the rotation frequency of Jupiter, x is the cylindrical distance of P from the rotation axis of Jupiter, G is the gravitational constant, and M is the mass of Jupiter (note that the gravitational potential is very small compared with the other terms). For the field line threading point P, $x_{\max}$ and r_0 are the distances of the centrifugal equator from the rotation axis and from the center of Jupiter, respectively.

[53] Solving the set of equations using Newton's method, we pose

$$F^{(0)} = \sum_{\alpha}^{N} n_\alpha\left(\phi_E^{(0)}\right) Z_\alpha \tag{A3}$$

and obtain the electric potential ϕ_E by iteration of

$$\phi_E^{(n+1)} = \phi_E^{(n)} + F^{(n)} \Big/ \left(\partial F^{(n)} / \partial \phi_E^{(n)}\right) \tag{A4}$$

For bi-Maxwellian distributions the convergence is very rapid ($\partial F/\partial\phi_E$ is linear). The bi-kappa distributions require $\sim$25 iterations to converge. The electric ambipolar potential ϕ_E is typically on the order approximately -50 V at 9 R_J and 10° centrifugal latitude. We show in Figure A2 the isocontours of ϕ_E as found for the density/temperature models of Figures 7, 8, and 9 (left-hand column).

[54] Finally, note that the kappa thermal speeds $\Theta_\parallel$ (needed for solving (10)) are derived from the parallel and perpendicular temperatures of the core and halo components of the ions n_c, T_c, n_h and T_h, using

$$\frac{m\Theta_\perp^2}{2k_B}\frac{\kappa}{\kappa - 3/2} = \frac{n_c T_c + n_h T_h}{n_c + n_h}, \tag{A5}$$

and that $A_0 = \Theta_\perp^2 \Big/ \Theta_\parallel^2$.

[55] **Acknowledgments.** F. B. is grateful to M. M. and N. M.-V. for their hospitality and to the University of Paris (Paris VII) for support while visiting l'Observatoire de Paris, Meudon, and acknowledges support from NASA through a grant under the Galileo Project (JPL contract 959550).

[56] Michel Blanc thanks the two referees for their assistance in evaluating this paper.

References

Bagenal, F., Empirical model of the Io plasma torus: Voyager measurements, *J. Geophys. Res.*, *99*, 11,043–11,062, 1994.

Bagenal, F., and J. D. Sullivan, Direct plasma measurements in the Io torus and inner magnetosphere of Jupiter, *J. Geophys. Res.*, *86*, 8447–8466, 1981.

Bagenal, F., F. J. Crary, A. I. F. Stewart, N. M. Schneider, D. A. Gurnett, W. S. Kurth, L. A. Frank, and W. R. Paterson, Galileo measurements of plasma density in the Io torus, *Geophys. Res. Lett.*, *24*, 2119–2122, 1997.

Belcher, J. W., The low-energy plasma in the Jovian magnetosphere, in *Physics of the Jovian Magnetosphere*, edited by A. J. Dessler, pp. 68–105, Cambridge Univ. Press, New York, 1983.

Collier, M. R., and D. C. Hamilton, The relationship between kappa and temperature in energetic ion spectra at Jupiter, *Geophys. Res. Lett.*, *22*, 303–306, 1995.

Connerney, J. E. P., Doing more with Jupiter's magnetic field, in *Planetary Radio Emissions III*, Austrian Acad. of Sci., Vienna, 1992.

Crary, F. J., F. Bagenal, J. A. Ansher, D. A. Gurnett, and W. S. Kurth, Anisotropy and proton density in the Io plasma torus derived from whistler wave dispersion, *J. Geophys. Res.*, *101*, 2699–2706, 1996.

Crary, F. J., F. Bagenal, L. A. Frank, and W. R. Paterson, Galileo plasma spectrometer measurements of composition and temperature in the Io plasma torus, *J. Geophys. Res.*, *103*, 29,359–29,370, 1998.

Divine, N., and H. B. Garrett, Charged particle distributions in Jupiter's magnetosphere, *J. Geophys. Res.*, *88*, 6889–6903, 1983.

Frank, L. A., and W. R. Paterson, Observations of plasmas in the Io torus with the Galileo spacecraft, *J. Geophys. Res.*, *105*, 16,017–16,034, 2000.

Frank, L. A., et al., Plasma observations at Io with the Galileo spacecraft, *Science*, *274*, 394–395, 1996.

Gurnett, D. A., et al., Galileo plasma wave observations in the Io plasma torus and near Io, *Science*, *274*, 391–392, 1996.

Herbert, F., and B. R. Sandel, Radial profiles of ion density and parallel temperature in the Io plasma torus during the Voyager 1 encounter, *J. Geophys. Res.*, *100*, 19,513–19,529, 1995.

Hill, T. W., Corotation lag in Jupiter's magnetosphere: Comparison of observation and theory, *Science*, *207*, 301–302, 1980.

Hill, T. W., A. J. Dessler, and F. C. Michel, Configuration of the Jovian magnetosphere, *Geophys. Res. Lett.*, *1*, 3–6, 1974.

Hoang, S., N. Meyer-Vernet, M. Moncuquet, A. Lecacheux, and B. M. Pedersen, Electron density and temperature in the Io plasma torus from Ulysses thermal noise measurements, *Planet. Space Sci.*, *41*, 1011–1020, 1993.

Huang, T. S., and T. J. Birmingham, The polarization electric field and its effect in an anisotropic rotating plasma, *J. Geophys. Res.*, *97*, 1511–1519, 1992.

Meyer-Vernet, N., Large-scale structure of planetary environments: The importance of not being Maxwellian, *Planet. Space Sci.*, *49*, 247–260, 2001.

Meyer-Vernet, N., M. Moncuquet, and S. Hoang, Temperature inversion in the Io plasma torus, *Icarus*, *116*, 202–213, 1995.

Moncuquet, M., Ulysses in the Io plasma torus: Electron density and temperature have been measured and models should be revised, paper presented at 27th Annual DPS Meeting, Am. Astron. Soc., Hawaii, 9–13 October 1995.

Moncuquet, M., Equilibre et confinement du tore de plasma d'Io dans la magnétosphère de Jupiter, Ph.D. thesis, 176 pp., Univ. Denis Diderot, Paris, France, December 1997.

Moncuquet, M., N. Meyer-Vernet, and S. Hoang, Dispersion of electrostatic waves in the Io plasma torus and derived electron temperature, *J. Geophys. Res.*, *100*, 21,697–21,708, 1995.

Moncuquet, M., N. Meyer-Vernet, S. Hoang, R. J. Forsyth, and P. Canu, Detection of Bernstein wave forbidden bands in the Jovian magnetosphere: A new way to measure the electron density, *J. Geophys. Res.*, *102*, 2373–2380, 1997.

Sandel, B. R., et al., Extreme ultraviolet observations from Voyager 2 encounter with Jupiter, *Science*, *206*, 962–966, 1979.

Schneider, N. M., and J. T. Trauger, The structure of the Io torus, *Astrophys. J.*, *450*, 450–462, 1995.

Scudder, J. D., On the causes of temperature change in inhomogeneous low-density astrophysical plasmas, *Astrophys. J.*, *398*, 299–318, 1992a.

Scudder, J. D., Why all stars should possess circumstellar temperature inversions, *Astrophys. J.*, *398*, 319–349, 1992b.

Siscoe, G. L., and D. Summers, Centrifugally driven diffusion of iogenic plasma, *J. Geophys. Res.*, *86*, 8471–8479, 1981.

Sittler, E. C., and D. F. Strobel, Io plasma torus electrons: Voyager 1, *J. Geophys. Res.*, *92*, 5741–5762, 1987.

Smith, R. A., and D. F. Strobel, Energy partitioning in the Io plasma torus, *J. Geophys. Res.*, *90*, 9469–9493, 1985.

Summers, D., and R. M. Thorne, A new tool for analyzing microinstabilities in space plasma modeled by a generalized Lorentzian (kappa) distribution, *J. Geophys. Res.*, *97*, 16,827–16,832, 1992.

Thomas, N., The variability of the Io plasma torus, *J. Geophys. Res.*, *98*, 18,737–18,750, 1993.

Thomas, N., Ion temperatures in the Io plasma torus, *J. Geophys. Res.*, *100*, 7925–7935, 1995.

Thomas, N., and G. Lichtenberg, The latitudinal dependence of ion temperature in the Io plasma torus, *Geophys. Res. Lett.*, *24*, 1175–1178, 1997.

Vasyliunas, V. M., A survey of low-energy electrons in the evening sector of the magnetosphere with Ogo 1 and Ogo 3, *J. Geophys. Res.*, *73*, 2839–2885, 1968.

F. Bagenal, Department of Astrophysical, Planetary and Atmospheric Sciences, University of Colorado, 391, UCB, Boulder, CO 80309-0391, USA. (bagenal@lasp.colorado.edu)

N. Meyer-Vernet and M. Moncuquet, Département de Recherche Spatiale, Observatoire de Paris-Meudon, 5 place Jules Janssen, 92195 Meudon Cedex, France. (nicole.meyer@obspm.fr; michel.moncuquet@obspm.fr)

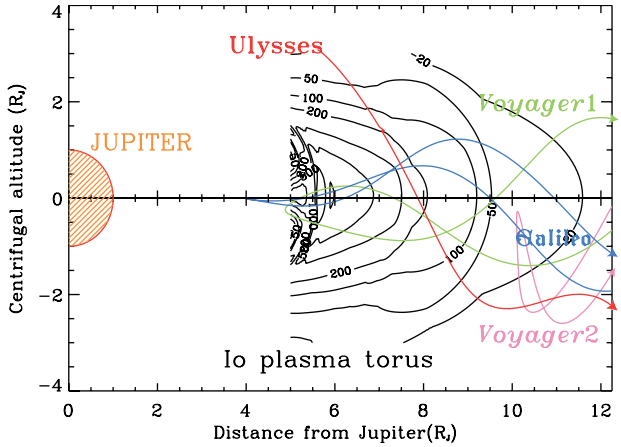

Figure 1. The trajectories of four spacecraft that have flown through the Io torus: Voyager 1 (green), Voyager 2 (pink), Ulysses (red), and Galileo's initial orbit (blue). The contours show electron density from the model of *Bagenal* [1994] (isotropic case with O_6 magnetic field model and no current sheet).

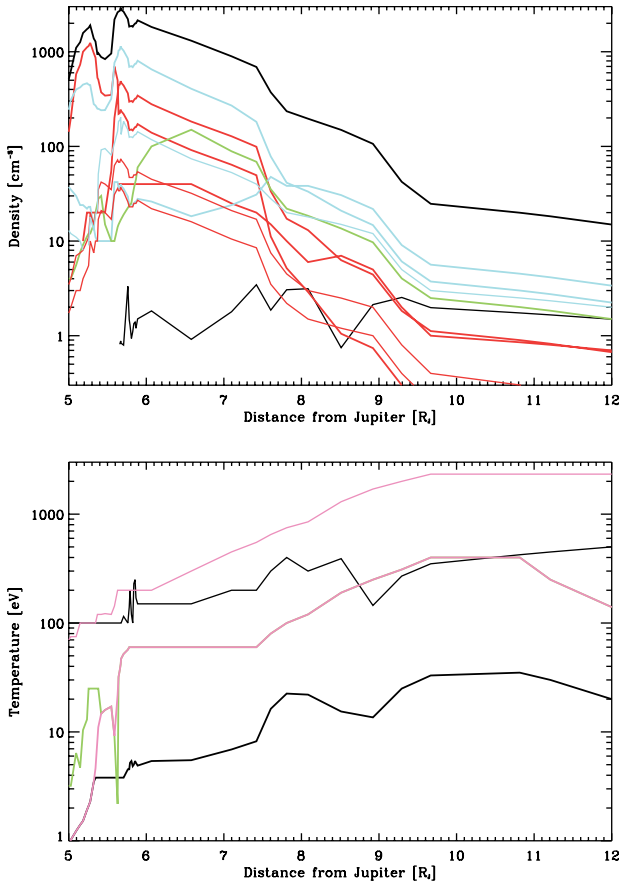

Figure 4. (top) Reference densities and (bottom) temperatures of the main particle species (from Voyager 1) used to compute our torus model (identical to *Bagenal* [1994]). The electron parameters are plotted in black, the densities of sulfur ions ($S^{+,\ ++,\ +++}$) are in red, and the densities of oxygen ions ($O^{+,\ ++}$) are in blue; the proton densities are plotted in green. The parameters of cold species (core) are plotted as bold lines and the parameters of hot species (halo) are plotted as thin lines (there is no halo for minor species S^{+++}, O^{++}, and protons). The core and halo temperatures (pink) are the same for all ions (except for the protons between 5 and 6 R_J, which are green).

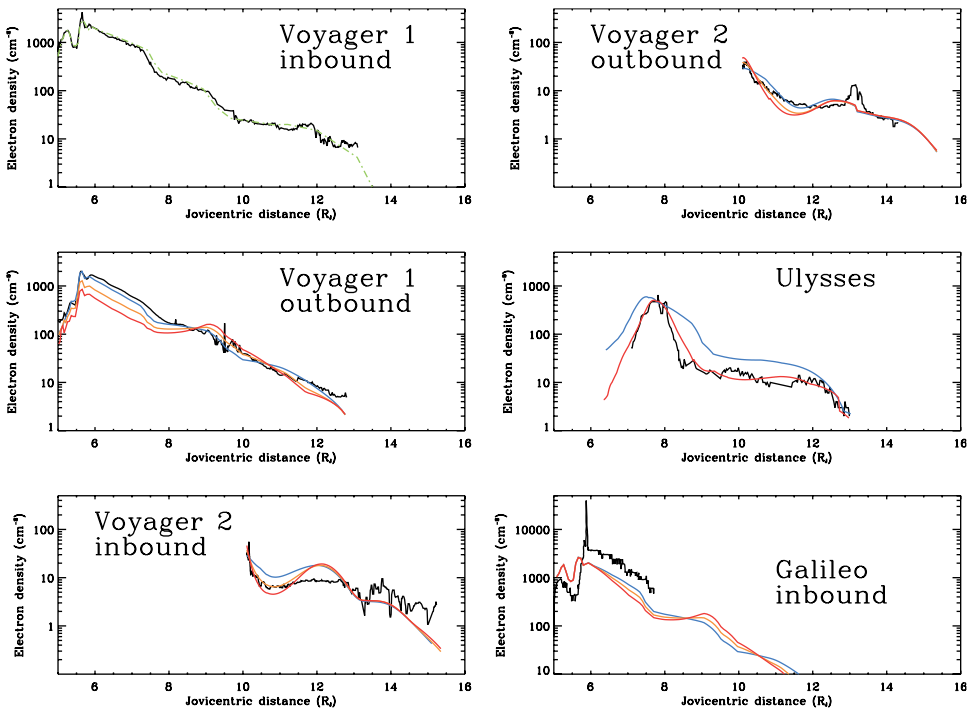

Figure 5. Comparison of computed models (colored lines) with measurements (black lines) of electron density from Voyager 1 and 2, Ulysses, and Galileo. The Voyager 1 inbound density profile is shown only with the reference data set (dash-dotted green line), which is used for building the other profiles. The predicted profiles have been superposed on the data: blue for the Maxwellian isotropic model; orange for the bi-kappa model with $\kappa_i = 2$, $\kappa_e = 2.4$, $A_{0i} = A_{0e} = 1.2$; and red for the bi-kappa model with $A_{0i} = 3$ and all other parameters as above. (Note that for Ulysses the density profiles have been multiplied by 1.9. The log-vertical (density) ranges are not the same for all panels.)

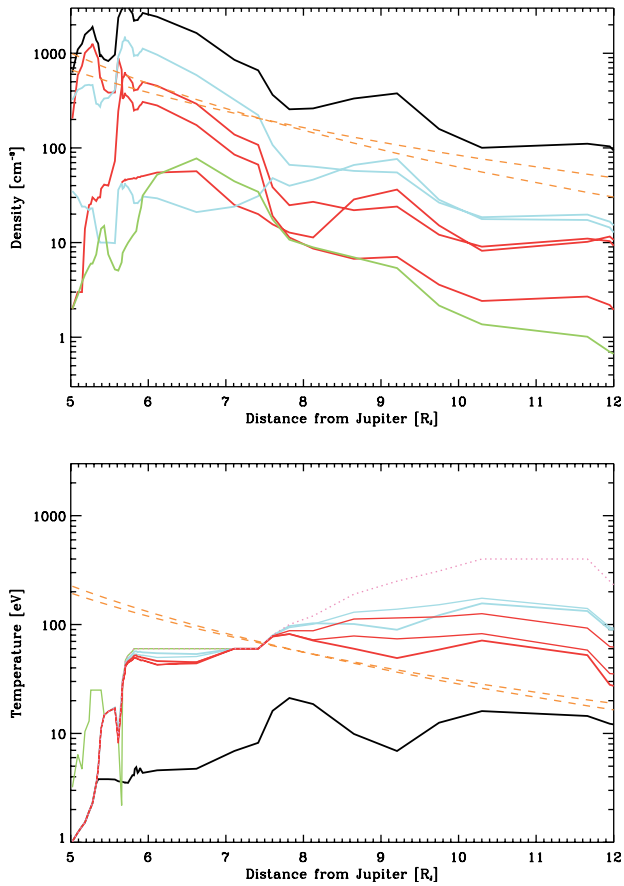

Figure 6. (top) Total densities and (bottom) perpendicular temperatures extrapolated from Voyager 1 to the centrifugal equator, using a bi-kappa function velocity distribution for the particles ($\kappa \equiv 2$ and $A_0 \equiv 3$ for *all* the ions; $\kappa_e = 2.4$ and $A_{0e} = 1.2$ for the electrons). Electrons are in black, sulfur is in red, oxygen is in blue, and protons are in green. We have superposed the former core plus halo ion temperature (pink dotted line) and adiabatic gradients (orange dashed lines) decreasing as L^{-4} or as L^{-3} for the densities and as $L^{-8/3}$ or as L^{-3} for the temperatures.

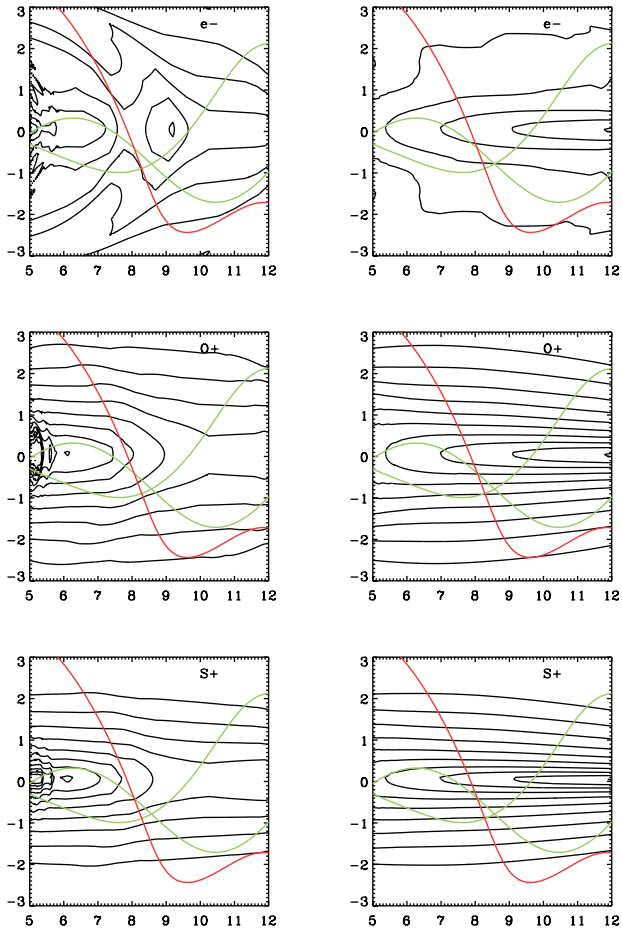

Figure 9. (left) Contours of temperature for electrons (e^-), S^+, and O^+ in the meridian plane for IAU System III longitude of 292°. The x axis gives distance from Jupiter (R_J), the y axis gives centrifugal altitude (R_J), $\kappa_i = 2$, $A_{0i} = 3$, $\kappa_e = 2.4$, and $A_{0e} = 1.2$. All contour levels are spaced by a factor of 2. The electron contours increase from 1 eV. The ions contours increase from 10 eV. (right) Temperature contours assuming an adiabatic L dependence at the centrifugal equator of L^{-3} (orange line in Figure 6). Colored curves are the trajectories of Ulysses (red) and of Voyager 1 (green).